Proceedings of the 8th U.S. National Conference on Earthquake Engineering
April 18-22, 2006, San Francisco, California, USA
Paper No. 89

LIQUEMAP:
A REAL-TIME POST-EARTHQUAKE MAP OF LIQUEFACTION PROBABILITY

T. L. Holzer[1], J.L. Blair[1], T.E. Noce[1], M.J. Bennett[1]

ABSTRACT

LiqueMap is a proposed map for real-time distribution over the internet that estimates the spatial distribution of liquefaction probability in the epicentral area immediately after an earthquake. As proposed here, it is based on the methodology for liquefaction hazard mapping that uses field-determined cumulative frequency distributions of the liquefaction potential index (LPI) of surficial geologic units to estimate the probability of surface manifestations of liquefaction at a given level of shaking and earthquake magnitude. The requirements for creating a LiqueMap after an earthquake are: (1) a map of PGA; (2) a map of the surficial geology; and (3) predetermined empirical LPI cumulative frequency distributions of the mapped surficial geologic units. LiqueMap as proposed here is generated by using a post-earthquake map of PGA and the LPI cumulative frequency distributions to map the probability of surface manifestations of liquefaction within the strongly shaken area. LiqueMap is potentially useful to utility and transportation agencies for assessing potential damage to lifelines from liquefaction-induced permanent ground deformation. When overlain on maps of vulnerable pipelines and other lifelines, LiqueMap can help set priorities for post-earthquake inspections.

Introduction

Modern internet technology increasingly is being applied to post-earthquake responses. These applications include not only rapid post-event determination and notification of the magnitude and location of seismic events, but estimates of the distribution of strong ground shaking. An example of the latter includes the posting by the U.S. Geological Survey of web-based maps, which are known as ShakeMaps, within minutes after an earthquake (Wald et al. 1999). These maps portray both the intensity of shaking and measured peak ground acceleration. In this paper, we propose a supplement to maps like ShakeMap. The supplemental map estimates in real time the spatial distribution of the probability of surface manifestations of liquefaction in areas of strong shaking. This map, which we will refer to as LiqueMap, can use the output from maps like ShakeMap as input. LiqueMap has a variety of potential applications

[1]Geologist, U.S. Geological Survey, MS 977, 345 Middlefield Road, Menlo Park, CA 94025

in addition to simply indicating areas where liquefaction is likely. It can be used by agencies concerned with the performance of lifelines, such as subgrade utilities and bridges to set priorities for post-earthquake safety inspections as well as input to loss models to improve estimates of earthquake loss. In this paper we describe a process to prepare a LiqueMap and illustrate LiqueMap with three earthquake scenarios that might strongly shake the sandy artificial fills in San Francisco Bay near Oakland, California (Fig. 1).

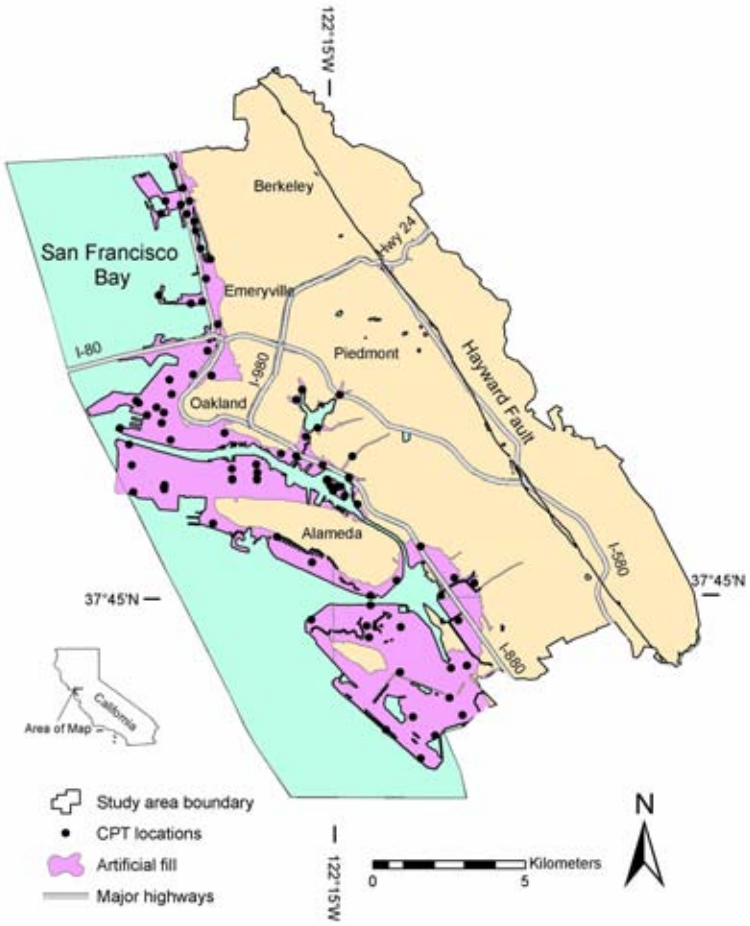

Figure 1. Area of artificial fill in the greater Oakland area and locations of CPT soundings used to estimate liquefaction probabilities for scenario earthquakes. Sounding data are available at http//:quake.usgs.gov/prepare/alameda.html. Fill area from Helley and Graymer (1997).

Methodology

LiqueMap as proposed here describes the spatial distribution of the probability of surface manifestations of liquefaction after an earthquake. Its feasibility rests on the widespread availability and power of geographic information systems and a recent advance in liquefaction hazard mapping that quantifies the spatial liquefaction hazard. This advance applies the liquefaction potential index (LPI), which was originally defined by Iwasaki et al. (1978, 1982) to predict liquefaction severity. In liquefaction hazard mapping, Holzer, Bennett et al. (2006) and

Holzer, Blair et al. (2006) have used LPI to predict the probability (or percent area) of surface manifestations of liquefaction. LPI and its application to hazard mapping are briefly summarized here.

LPI, which is evaluated at a specific location, weighs factors of safety and thickness of potentially liquefiable layers according to depth. In the application here, LPI values are computed from cone penetration test (CPT) soundings. LPI assumes that the severity of liquefaction is proportional to:

1. cumulative thickness of the liquefied layers;
2. proximity of liquefied layers to the surface; and
3. amount by which the factor safety (FS) is less than 1.0, where FS is the ratio of soil capacity to resist liquefaction to seismic demand imposed by the earthquake, i.e., the ratio of cyclic resistance ratio to the cyclic stress ratio.

Iwasaki (1978) defined the index as:

$$LPI = \int_0^{20m} F\, w(z)\, dz \qquad (1)$$

where

$$F = 1 - FS \quad \text{for } FS \leq 1 \qquad (2a)$$

$$F = 0 \quad \text{for } FS > 1 \qquad (2b)$$

$$w(z) = 10 - 0.5\, z, \text{ where } z \text{ is the depth in meters.} \qquad (2c)$$

For hazard mapping, Holzer, Bennett et al. (2006) and Holzer, Blair et al. (2006) use the FS as defined in the Seed-Idriss simplified procedure (Seed and Idriss 1971; Seed et al. 1985; Youd et al. 2001) as modified for the CPT by Robertson and Wride (1997).

Iwasaki et al. (1982) and Toprak and Holzer (2003) independently determined the significance of LPI values. Both groups compiled case histories and correlated LPI with the observed severity of liquefaction. Iwasaki et al. (1982) concluded that severe liquefaction is likely at sites with LPI>15 and that severe liquefaction is unlikely at sites with LPI<5. Severity was defined in terms of foundation damage. Their computations of LPI relied on blow counts from standard penetration tests and a FS defined by Iwasaki et al. (1982). Toprak and Holzer (2003) computed LPI values from cone penetration test (CPT) soundings at sites with surface manifestations of liquefaction during the 1989 Loma Prieta, California, earthquake, and concluded that sand boils typically occurred at soundings where LPI≥5 and lateral spreads typically occurred where LPI≥12. These thresholds are based on median LPI values. Lower and upper quartiles were 3 and 10 for sand boils and 5 and 17 for lateral spreads.

To calculate probabilities of surface manifestations of liquefaction for a mapped geologic unit using the methodology of Holzer, Bennett et al. (2006), the variability of LPI within the area underlain by the unit must be determined. This is done by conducting multiple CPT soundings in the mapped unit and then computing an LPI value for each sounding for a given earthquake magnitude and peak ground acceleration (PGA). If the spacing of the CPT soundings are

approximately uniform in the geologic unit and the unit is spatially heterogeneous, the cumulative percentage or frequency of LPI values greater than or equal to 5 can be interpreted as the probability that surface manifestations of liquefaction at the specified PGA. This frequency also can be interpreted as a percent of the total surface area that will exhibit surface manifestations of liquefaction if the area is shaken at a uniform PGA.

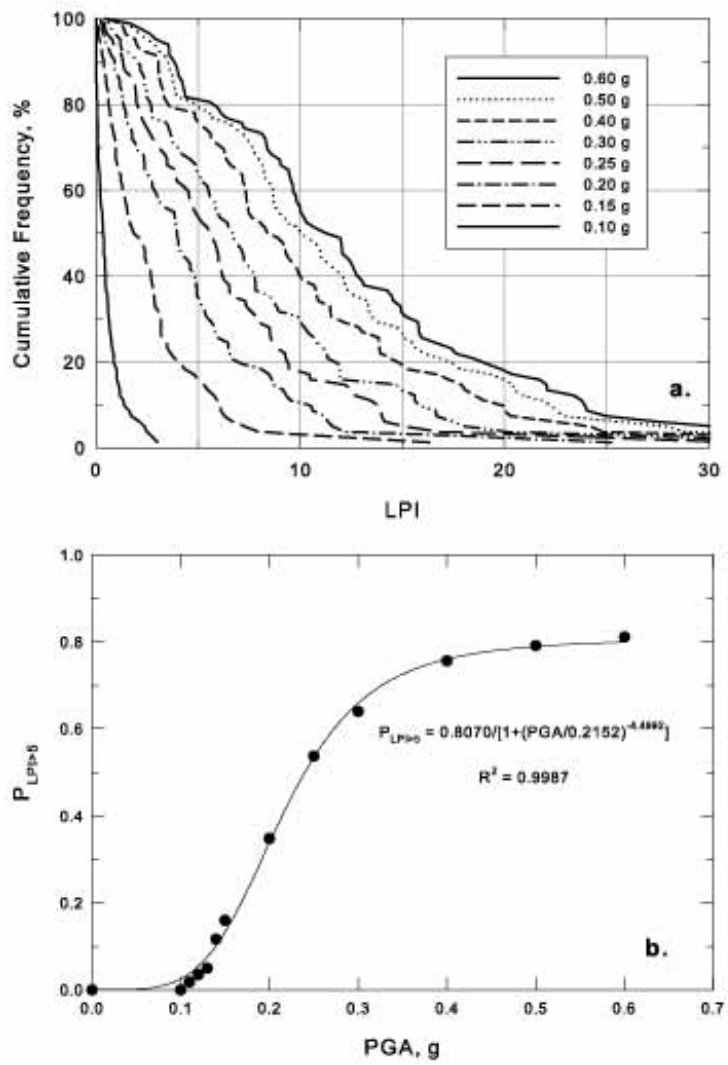

Figure 2. (**a.**) Cumulative frequency distributions of LPI for East Bay artificial fills for M7.8 earthquake and different PGA values; (**b.**) Probability of surface manifestations of liquefaction versus PGA (M=7.8) for East Bay fills determined from LPI=5 in **a**. Probabilities were fit with a 4-parameter logistic curve. Cumulative frequency distributions are not shown in **a.** for PGA ranging from 0.11 to 0.14 g.

To illustrate the calculation of probability, consider the area underlain by sandy artificial fills that were placed into San Francisco Bay near Oakland California (Fig. 1). Subsurface conditions in the area were previously documented with 82 CPT soundings by the USGS

(Holzer, Bennett et al. 2006, Holzer et al. 2005). Assume the area is shaken by a M7.8 earthquake and the spatial variation of PGA is known. First LPI values must be computed for each CPT sounding for different PGA values caused by the M7.8 earthquake and then cumulative frequency distributions of LPI for each PGA must be compiled (Fig. 2a). The cumulative frequency at LPI=5 for each distribution in Fig. 2a is the probability of surface manifestations of liquefaction in the artificial fill at the given PGA. By plotting this probability versus PGA, the probability of surface manifestations of liquefaction can be inferred from PGA for the M7.8 earthquake (Fig. 2b).

To facilitate the routine production of a LiqueMap after an earthquake, it may be useful to compute the liquefaction probabilities beforehand for a range of earthquake magnitudes and PGA values and summarize them in a look-up table. Table 1 is a possible format for such a table. Probabilities for intermediate values of magnitude and PGA can be interpolated from the table.

Table 1. Probability of surface manifestations of liquefaction of sandy artificial fills along the eastern shore of San Francisco Bay near Oakland, California. See Fig. 1 for location.

PGA, g	M8	M7.5	M7	M6.5	M6	M5.5	M5
0	0	0	0	0	0	0	0
0.10	0	0	0	0	0	0	0
0.15	0.18	0.08	0.03	0	0	0	0
0.20	0.42	0.26	0.17	0.04	0	0	0
0.25	0.57	0.47	0.30	0.18	0.05	0	0
0.30	0.67	0.58	0.48	0.28	0.17	0.04	0
0.40	0.76	0.69	0.64	0.53	0.38	0.20	0.05
0.50	0.78	0.76	0.72	0.66	0.54	0.40	0.18
0.60	0.79	0.78	0.77	0.71	0.65	0.54	0.30

LiqueMap

Examples of LiqueMap were prepared for three earthquake scenarios that are likely to produce liquefaction of the artificial fills shown in Fig. 1. The artificial fills extend from the City of Berkeley southward to the Cities of Oakland and Alameda along the eastern margin of San Francisco Bay, California. These sandy artificial fills underlie 57 km^2 of made ground along the shoreline (Fig. 1). Most of this fill was emplaced by either hydraulic dredging or placement from land into water. It was mostly emplaced in the six decades after the 1906 San Francisco earthquake and has been significantly shaken only once by an earthquake; PGA equaled approximately 0.2 g during the 1989 Loma Prieta M6.9 earthquake (Brady and Shakal 1998).

Values of PGA for each earthquake scenario presented here were computed with the ground motion prediction (attenuation) equation (GMPE) of Boore et al. (1997). PGA values with this GMPE are determined by earthquake magnitude, style of faulting, distance from the fault, and local site conditions. Only strike-slip style fault events were considered here. Boore et al. (1997) use V_{S30} to parameterize site conditions, where V_{S30} is the average shear wave velocity to a depth of 30 m. It is computed by dividing 30 m by the travel time of a vertically propagating

shear wave. PGA values were computed at nodes in a 50-m grid. The V_{S30} used at each node in the 50-m grid was from Holzer et al. (2005). The computational procedure for estimating PGA is described more completely in Holzer, Blair et al. (2006). To implement an actual LiqueMap, we would expect that the spatial variation of PGA would be inferred from measured values.

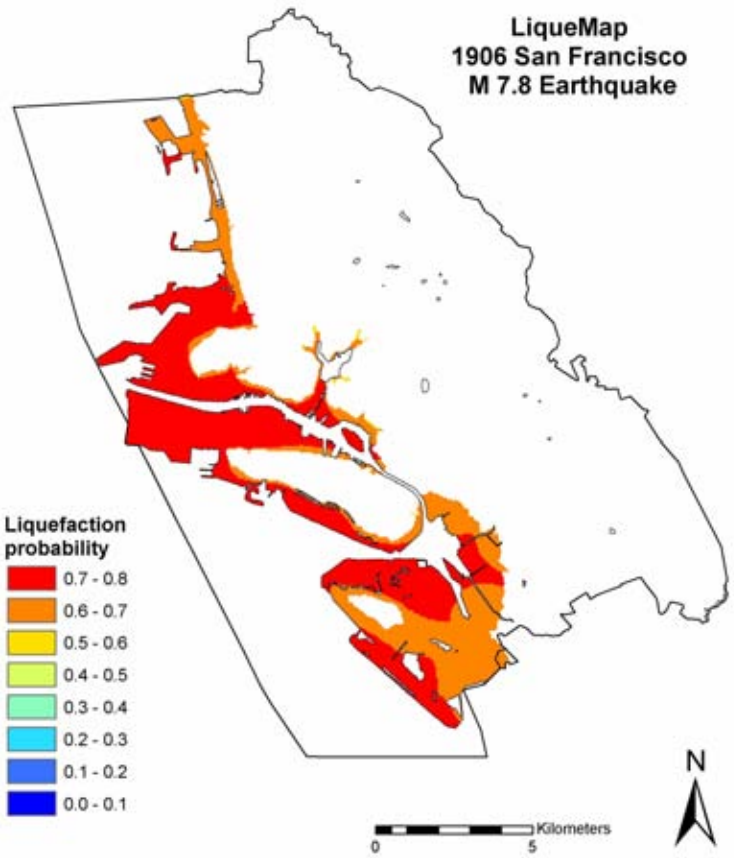

Figure 3. LiqueMap for a repeat of the 1906 San Francisco M7.8 earthquake, which ruptured the San Andreas Fault 18-26 km west of the area of artificial fill.

Fig. 3 is a LiqueMap for a repeat of a 1906 San Francisco M7.8 earthquake. The 1906 earthquake was on the San Andreas Fault and lies 18 to 26 km southeast of the area of artificial fill. The probabilities are based on median PGA values predicted by the Boore et al. (1997) GMPE. The LiqueMap for a repeat of this earthquake predicts significant liquefaction in all of the fill area. Probabilities decrease slightly in the eastern part of the fill owing to a decrease of PGA. The decrease of PGA is caused by both an increase of V_{S30}, which reduces site amplification, and greater distance from the San Andreas Fault.

Fig. 4 is a LiqueMap for a M6.9 earthquake on the nearby Hayward Fault, which is shown in Fig. 1. It too is based on median predicted PGA. The fills are from 4 to 12 km from the fault. They average about 9 km in southern part of the study area. Although liquefaction

probabilities are greater than 0.5 throughout the area of fill, probabilities decrease slightly from east to west, reflecting a decrease of PGA. The tongue of increased probability on the north side of Alameda Island, the large island in the center of the map, is caused by a buried channel filled with low-velocity younger San Francisco Bay mud. The increased thickness of mud causes low values V_{S30} and greater predicted site amplification in this area.

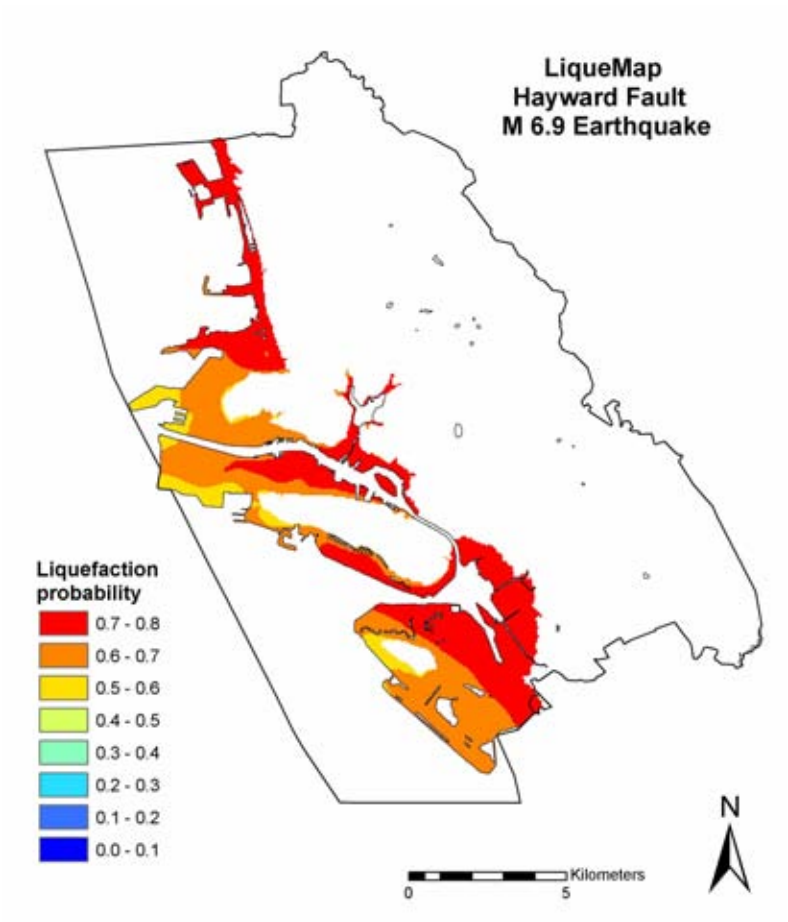

Figure 4. LiqueMap for a M6.9 earthquake on the nearby Hayward Fault.

Fig. 5 is a LiqueMap for the 1989 Loma Prieta M6.9 earthquake. The northwestern end of the seismic source zone of the1989 earthquake ranged from approximately 70 to 90 km south-southeast of the area of artificial fill, but nevertheless caused significant damage in the San Francisco and Oakland area. PGA values recorded in the areas of fill were approximately 0.2 g (Brady and Shakal 1998). The earthquake caused widespread liquefaction in the East Bay artificial fill (see Fig. 5). Probabilities of liquefaction are significantly less for the Loma Prieta earthquake than for the Hayward Fault earthquake, despite both having the same magnitude 6.9. The difference is primarily attributable to the greater distance of the fill area from the Loma Prieta earthquake source zone. Despite the increased distance from the earthquake source as one moves northward in the study area, east-west tongues of higher probability are conspicuous in the LiqueMap. These areas overlie the buried channels filled with younger bay mud that have the potential to locally amplify ground motion.

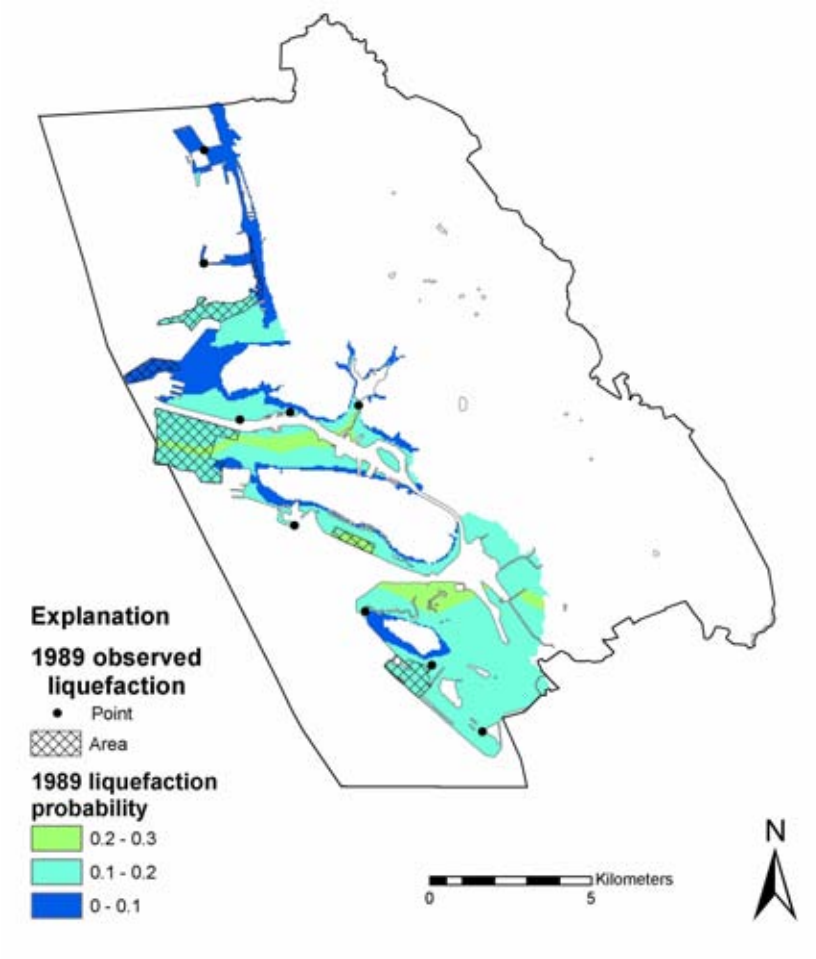

Figure 5. LiqueMap for the 1989 Loma Prieta M6.9 earthquake on a segment of the San Andreas Fault, approximately 70 to 90 km southwest of study area. Areas of observed liquefaction are from Tinsley et al. (1998).

Conclusions

At this stage of its development, LiqueMap is primarily a proposed method to depict probabilities of surface manifestation of liquefaction probabilities in real time after an earthquake. It has not been implemented. Two basic challenges confront the implementation of LiqueMap: (1) realistic resolution of the spatial variation of ground motion during an earthquake and (2) information on the relation between liquefaction probability and ground motion.

In the United States, ShakeMap is currently the state-of-the-art tool for predicting the spatial distribution of ground motion after an earthquake (Wald et al. 1999). The reliability of ground motion estimates by ShakeMap, however, depends on the density of the ground-motion observation network. Liquefaction most commonly occurs and is severest in areas underlain by

artificial fill and younger Holocene sediments such as in floodplains and estuaries. These settings are also the provenance of local site effects, which can cause significant spatial variability of ground motion over short distances. Dense networks of ground motion recording stations typically are required in these areas to reliably determine ground motion. In other words, the reliability of the liquefaction predictions will depend strongly on the reliability of the post-earthquakes estimates of ground motion.

The other requirement for LiqueMap is knowledge of the relation between liquefaction probability and ground motion for each of the surficial geologic units in the area of strong shaking. With the methodology proposed here, this requires documentation of the statistical distributions of LPI of mapped surficial geologic units. While we advocate the use of multiple CPT soundings or standard penetration test (SPT) borings that meet the standards for liquefaction analyses (Seed et al. 1985), this may not always be feasible. In many cases, one might be forced to rely on previously conducted commercial borings, the quality and distribution of which can be highly variable.

Acknowledgments

We appreciate reviews by David K. Keefer and John C. Tinsley, III.

References

Boore, D.M., Joyner, W.B., and Fumal, T.E., 1997. Empirical near-source attenuation relations for horizontal and vertical components of peak ground acceleration, peak ground velocity, and pseudo-absolute acceleration response spectra, *Seismol. Res. Lett*., 68 (1), 154-179.

Brady, A.G., and Shakal, A.F., 1998. Strong-motion recordings, *in* Borcherdt, R.D., ed., The Loma Prieta, California, earthquake of October 17, 1989 - Strong ground motion, *U. S. Geological Survey Professional Paper 1551-A*, pp. A9-A38.

Helley, E.J., and Graymer, R.W., 1997. Quaternary geology of Alameda County, and parts of Contra Costa, Santa Clara, San Mateo, San Francisco, Stanislaus, and San Joaquin Counties, California, A digital database, *U.S. Geol. Surv. Open-file Rpt. 97*-97 (http://wrgis.wr.usgs.gov/open-file/of97-97/).

Holzer, T.L., Bennett, M.J., Noce, T.E., Padovani, A.C., and Tinsley, J.C., III, 2006. Liquefaction hazard mapping with LPI in the greater Oakland, California, area, *Earthquake Spectra*, 22 (3), in press.

Holzer, T.L., Blair, J.L., Noce, T.E., and Bennett, M.J., 2006. Predicted liquefaction of east bay fills during a repeat of a 1906 earthquake, *Earthquake Spectra Commemorative Theme Issue on the 1906 San Francisco Earthquake*, EERI, in press.

Holzer, T.L., Padovani, A.C., Bennett, M.J., Noce, T.E., and Tinsley, J.C., III, 2005. Mapping NEHRP V_{S30} site classes, *Earthquake Spectra*, 21 (2), 353-370.

Iwasaki, T., Tatsuoka, F., Tokida, K.-i., and Yasuda, S., 1978. A practical method for assessing soil liquefaction potential based on case studies at various sites, in *Proceedings, Second International Conference on Microzonation*, San Francisco, pp. 885-896.

Iwasaki, T., Tokida, K., Tatsuoka, F., Watanabe, S., Yasuda, S., and Sato, H., 1982. Microzonation for soil liquefaction potential using simplified methods, in *Proceedings Third International Earthquake Microzonation Conference*, Seattle, pp. 1319-1330.

Robertson, P.K., and Wride, C.E., 1997. Cyclic liquefaction and its evaluation based on the SPT and CPT, in *Proceedings, Evaluation of liquefaction resistance of soils*, T.L. Youd and I.M. Idriss

(editors), *National Center for Earthquake Engineering Research Tech. Rept. NCEER-97-0022*, pp. 41-87.

Seed, H.B., and Idriss, I.M., 1971. Simplified procedure for evaluating soil liquefaction potential, *J. Soil Mech. Found. Eng.* 97 (9), 1249-1273.

Seed, H.B., Tokimatsu, K., Harder, L.F., and Chung, R.M., 1985. Influence of SPT procedures in soil liquefaction resistance evaluations, *J. Geotech. Eng.* 111 (12), 1425-1445.

Tinsley, J.C., III, Egan, J.A., Kayen, R.E., Bennett, M.J., Kropp, A., and Holzer, T.L., 1998. Appendix: Maps and descriptions of liquefaction and associated effects, *in* Holzer, T.L., ed., The Loma Prieta, California, earthquake of October 17, 1989 - Liquefaction, *U. S. Geological Survey Professional Paper 1551-B*, pp. B287-B314.

Toprak, S., and Holzer, T.L., 2003. Liquefaction potential index: Field assessment, *J. Geotech. Geoenviron. Eng.* 129 (4), 315-322.

Wald, D.A., Quitoriano, V., Heaton, T.H., Scrivner, C.W. and Worden, C.B., 1999. Trinet "ShakeMaps": Rapid generation of peak ground motion and intensity maps in California, *Earthquake Spectra*, 15 (3), 537-546.

Youd, T.L., and Idriss, I.M., Andrus, R.D. Arango, I., Castro, G., Christian, J.T., Dobry, R., Liam Finn, W.D.L., Harder, L.F., Jr., Hynes, M.E., Ishihara, K., Koester, J.P., Liao, S.S.C., Marcuson, W.F., III, Martin, G.R., Mitchell, J.K., Moriwaki, Y., Power, M.S., Robertson, P.K., Seed, R.B., Stokoe, K.H., II, 2001. Liquefaction resistance of soils: Summary report from the 1996 NCEER and 1998 NCEER/NSF workshops on evaluation of liquefaction resistance of soils, *J. Geotech. Geoenviron. Eng.* 127 (10), 817-833.